Vertical Geometry, 2-A Forward Current Ga_2O_3 Schottky Rectifiers on Bulk Ga_2O_3 Substrates

Jiancheng Yang, Fan Ren, *Fellow, IEEE*, Steve J. Pearton, *Fellow, IEEE*, and Akito Kuramata

***Abstract*— Large area (up to 0.2 cm^2) Ga_2O_3 rectifiers without edge termination were fabricated on a Si-doped n-Ga_2O_3 drift layer grown by halide vapor phase epitaxy on a Sn-doped n$^+$$Ga_2O_3$ (001) substrate. A forward current of 2.2 A was achieved in single-sweep voltage mode, a record for Ga_2O_3 rectifiers. The on-state resistance was 0.26 $\Omega \cdot$ cm^2 for these largest diodes, decreasing to 5.9 $\times$ 10^{-4}$\Omega \cdot$ cm^2 for 40 $\times$ 40 μm^2 devices. The temperature dependence (25 °C–125 °C) of forward current density was used to extract the barrier height of 1.08 eV for Ni and a Richardson's constant of 48 A $\cdot$ cm^{-2} $\cdot$ K^{-2}. Ideality factors were in the range 1.01–1.05, with the barrier height decreasing with temperature. The reverse breakdown was a strong function of diode area, decreasing from 466 V (1.6 $\times$ 10^{-5} cm^2) to 15 V for 0.2 cm^2. This led to power figure-of-merits (V_B^2/R_{ON}) in the range 3.68 $\times$ 10^8–865 W $\cdot$ cm^{-2} over this area range. The reverse breakdown voltage scaled approximately as the contact perimeter, indicating it was dominated by the surface and decreased with temperature with a negative temperature coefficient of 0.45 V $\cdot$ K^{-1}. The reverse recovery time when switching from +1 V to reverse bias was 34 ns.**

***Index Terms*— Forward current, gallium oxide, rectifiers, Schottky diode.**

I. Introduction

Ga_2O_3 is attracting significant interest for power electronics applications because of its large breakdown field of ~8 mV cm^{-1} [1]–[10]. This is well in excess of the values for SiC and GaN, both of which are now established with commercial availability of high power devices [11], [12] and thus the hope is that Ga_2O_3 devices could extend this performance on the high voltage, low frequency end. A thorough discussion of the relative power figure-of-merits has been given recently for all these materials [8]–[10]. Wide bandgap switches are attractive due to their increased tolerance to temperatures above the limits of silicon [11], [12]. Reduction of bulky, expensive cooling equipment should be possible, leading to decreased system complexity and cost [11], [12]. Other end-uses include electronic motor controls, lighting, heating, and air-conditioning. A key component of the inverter modules required for many of these applications is the rectifier, one of two most common devices for power conversion systems (rectifiers and field-effect transistors) and under development for Ga_2O_3 [13]–[30]. These have benefited from the recent advances in epitaxial growth technology for thick, low carrier concentration, homoepitaxial Ga_2O_3 drift layers. The wide bandgap of Ga_2O_3 allows it to sustain extremely high critical electric fields, leading to large blocking voltages in these power rectifiers [3], [8], [10]. There are also recent advances in edge termination methods that reduce sharp regions of high electric field and can enhance the reverse breakdown voltage V_{BR}[19], [20]. A number of small area Ga_2O_3 rectifiers have demonstrated V_{BR} values in excess of 1 kV with near-ideal forward current–voltage (I–V) characteristics and reasonably low specific on-resistances, R_{on} [17]–[19]. Further improvement in the efficiency, footprint, and functionality of power systems will strongly rely on using new materials-like $Ga_2O_3$with intrinsic advantages and in particular, vertical structures offer advantages of small footprint, higher current conduction, and speed [7], [8], [10].

To date, there has been little study of large area Ga_2O_3 Schottky diode rectifiers of the type needed to achieve high absolute currents, not just current density. In this paper, we report on the size and temperature dependence (25 °C–125 °C) of electrical characteristics of vertical Ga_2O_3 diodes over a large range of areas (1.6 $\times$ 10^{-5}–0.2 cm^2). Maximum forward currents in single-sweep mode of 2.2 A are demonstrated. The reverse breakdown voltage is a strong function of diode area, showing the influence of defect density.

II. Experiment

The starting samples were bulk β-phase Ga_2O_3 single crystal wafers (~650 μm thick) with (001) surface orientation (Tamura Corporation, Sayama, Japan) grown by the edge-defined film-fed growth method. Hall effect measurements

Manuscript received February 27, 2018; revised April 16, 2018 and May 4, 2018; accepted May 16, 2018. Date of publication May 25, 2018; date of current version June 19, 2018. This work was supported in part by the Department of the Defense, Defense Threat Reduction Agency, monitored by Jacob Calkins under Grant HDTRA1-17-1-011, and in part by the New Energy and Industrial Technology Development Organization, Japan through this project "The Research and Development Project for Innovation Technique of Energy Conservation." The review of this paper was arranged by Editor B. Zhang. *(Corresponding author: S. J. Pearton.)*

J. Yang and F. Ren are with the Department of Chemical Engineering, University of Florida, Gainesville, FL 32611 USA.

S. J. Pearton is with Department of Materials Science and Engineering, University of Florida, Gainesville, FL 32611 USA (e-mail: spear@mse.ufl.edu).

A. Kuramata is with Tamura Corporation, Sayama, Saitama 350-1328, Japan, and also with Novel Crystal Technology, Inc., Sayama 350-1328, Japan.

Color versions of one or more of the figures in this paper are available online at http://ieeexplore.ieee.org.

Digital Object Identifier 10.1109/TED.2018.2838439

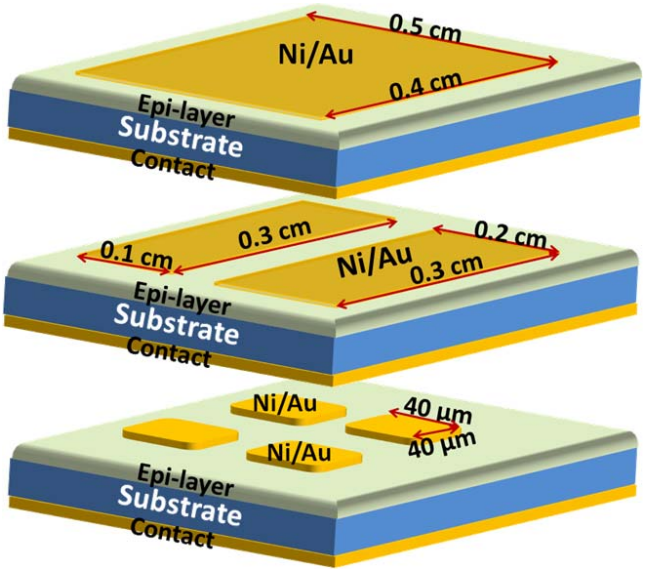

Fig. 1. Schematic of the three different device across-sections studied, with front side Ni/Au rectifying contacts and full area backside Ti/Au Ohmic contacts.

showed the Sn-doped samples had carrier concentration of 3.6×10^{18} cm^{-3}. Epitaxial layers (initially ~15 μm thick) of lightly Si-doped n-type Ga_2O_3 (~2×10^{16} cm^{-3}) were grown on these substrates by Hydride Vapor Phase Epitaxy at Novel Crystal Technology. After growth, the epi surface subjected to chemical mechanical polishing to remove pits [17], [18]. The final epi layer thickness was ~7 μm. The X-ray diffraction full-width at half maximum (FWHM) of the (402) peak was ~10 arc · s and the dislocation density from etch pit observation was of the order of 10^3 cm^{-2} and the X-ray diffraction FWHM was 137 arc · s. This correlates to a defect density in-plane of ~3×10^3 cm^{-2}.

The device geometries are shown in Fig. 1. Diodes were fabricated by depositing a full area back Ohmic contacts of Ti/Au (20/80 nm) by E-beam evaporation. The samples were treated in ozone for 15 min before Schottky metal deposition to remove the hydrocarbons and oxidize the surface. Ohmic behavior was achieved without the need for dry etching or ion implantation. The front sides were patterned by lift-off of E-beam deposited Schottky contacts Ni/Au (20/80 nm) on the epitaxial layers [17], [18]. Four different contact dimensions were employed, namely, 0.4×0.5 cm^2, 0.2×0.3 cm^2, 0.1×0.3 cm^2, and 40×40 μm^2. I–V characteristics were recorded in air at 25 °C–125 °C on a hot stage using either an Agilent 4145B parameter analyzer or a Tektronix 370-A curve tracer for high currents.

III. Results and Discussion

Both forward I–V and reverse I–V characteristics of the devices were measured by Agilent analyzer 4156 and Tektronix 370 A. For the reverse I–V voltage that is larger than 100 V and forward I–V current that is larger than 100 mA, the Tektronix 370 A instrument was used due to the voltage and current limitation of the Agilent analyzer 4156. Also, due to the measurement limitation on

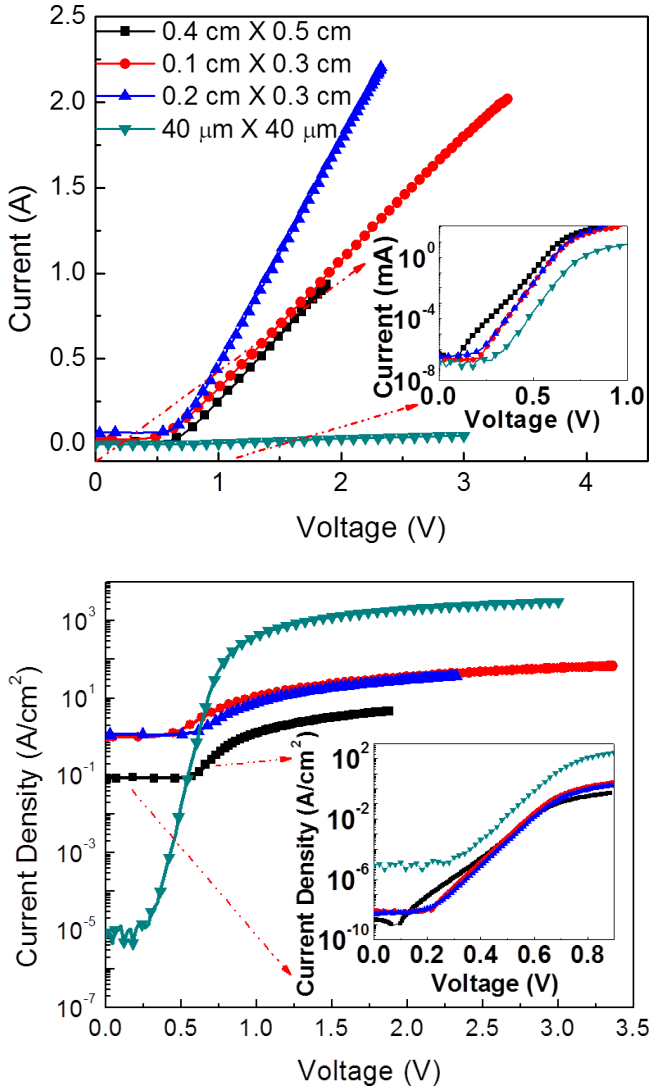

Fig. 2. Forward I–V characteristics of packaged Ga_2O_3 diodes of different rectifying contact dimension measured in Tektronix 370 A (main plot) and Agilent analyzer 4156 (inserts). Data is plotted in log form in the inset (top) and the current density characteristics from the same diodes (bottom).

Tektronix 370 A, Agilent analyzer 4156 was used for the measurements of current that is smaller than 100 mA. Fig. 2 shows the single sweep forward I–Vs for the four different geometry devices on both linear (top) and log (bottom) scales. Previous small area Ga_2O_3 rectifiers have achieved impressive reverse characteristics, but forward characteristics have always been reported as current density. These devices represent a large step toward the achievement of practical ON-state current levels [31]. Both the 0.2×0.3 and 0.1×0.3 cm^2 devices could be pushed to above 2 A, with a maximum of 2.2 A for the former. Since these were single sweeps, excessive self-heating was not a significant issue and the devices showed no degradation in performance. In sweep mode, the collector supply sweeps from 0 V to its preselected value. During the sweep, 1% duty cycle of a 280 μs pulsewidth was used. There were around 200 data points collected for each sweep. We were able to measure the devices under these types of

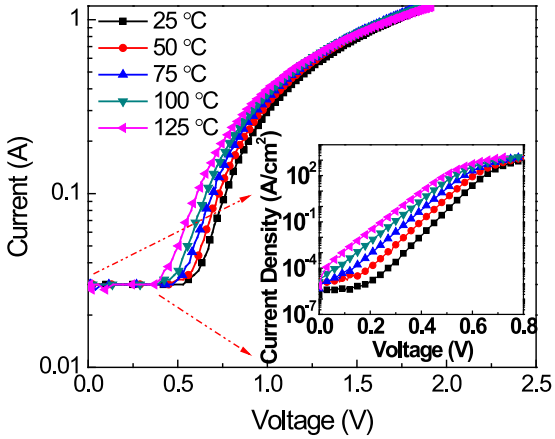

Fig. 3. Temperature dependence of forward current for a 0.2 × 0.3 cm^2 diode. Inset shows forward *I–V* of the low-voltage region.

TABLE I
SUMMARY OF DEVICE PARAMETERS FOR DIFFERENT CONTACT SIZES

Device Size	0.4 x 0.5 cm^2	0.2 x 0.3 cm^2	0.1 x 0.3 cm^2	40 x 40 μm^2
Device Area (cm^2)	0.2	0.06	0.03	1.65 x10^{-5}
Device Perimeter (cm)	1.8	1	0.8	1.60 x10^{-2}
Breakdown Voltage (V_B)	-15	-97	-100	-466
Schottky Barrier Height (eV)	0.97	1.07	1.08	1.08
Ideality Factor	1.18	1.03	1.02	1.03
On-Resistance (Ω.cm^2)	0.26	0.08	0.023	5.90 x10^{-4}
V_B^2/R_{ON} (W.cm^2)	865	1.18 x10^5	4.35x10^5	3.68 x10^8

condition over the hot stage temperatures from 25 °C–125 °C and do extensive testing without any hysteresis or degradation, showing the robustness of the Ga_2O_3 under these conditions. We have noted previously that permanent degradation of the Schottky contacts can occur for annealing temperatures above 450 °C [32]. The main plots are from the Tektronix 370 A and the inserts are from the Agilent 4156. The maximum current level for Agilent for 4156 allowed is 100 mA, and this can measure currents in the pA range. The Tektronix 370 A has the capability of measuring current in range. The current of the biggest diode is smaller than the smaller ones. This is due to the nonuniformity of Ga_2O_3 wafer, verified with CV measurements. The larger diode has a concentration of 9 × 10^{15} cm^{-3} and the carrier concentration of 0.1 cm × 0.3 cm diode was around to 2 × 10^{16} cm^{-3}. Thus, the small diode delivered a higher forward current.

Fig. 3 shows the temperature dependence of forward *I–V* characteristics from 25 °C to 125 °C for the 0.2 × 0.3 cm^2 diodes. The ideality factor (η) at each temperature was estimated by fitting the linear region of the *J–V* curve to the thermionic emission (TE) model [13]–[16]. An effective Schottky barrier height at zero bias ($e\Phi_{b0}$) can be calculated from the relation $e\Phi_{b0} = eV_{bi0} + (E_c - E_f) - \mathrm{e}\Delta\Phi_{\mathrm{ifbl0}}$. In this relation, e is the electronic charge, Φ_b is the barrier height, E_C is the conduction band minimum, E_f is the Fermi level, and the $\mathrm{e}\Delta\Phi_{ifbl0}$ term represents the image charge barrier lowering at zero bias. Using the same procedure as [16], we obtained near-ideal Schottky characteristics with η values of 1.02–1.18, depending on diode area. These are summarized in Table I. The breakdown voltage was defined with the reverse breakdown leakage current reaching 0.5 mA · cm^{-2}. Note that in Table I that normalized R_{on} is dependent on the size due to the metal resistance of the Schottky metal; 400 mΩ for 100 nm Ni/Au. This was the main reason for the lower Ron for 40 μm × 40 μm diode. The second reason was nonuniformity of the carrier concentration across the wafer ranging from 9 × 10^{15} to 2 × 10^{16} cm^{-3}.

Forward current conduction in all of our diodes was governed by TE as the dominant mechanism. The $q\phi_{\mathrm{b,0}}$ was determined from the forward current density

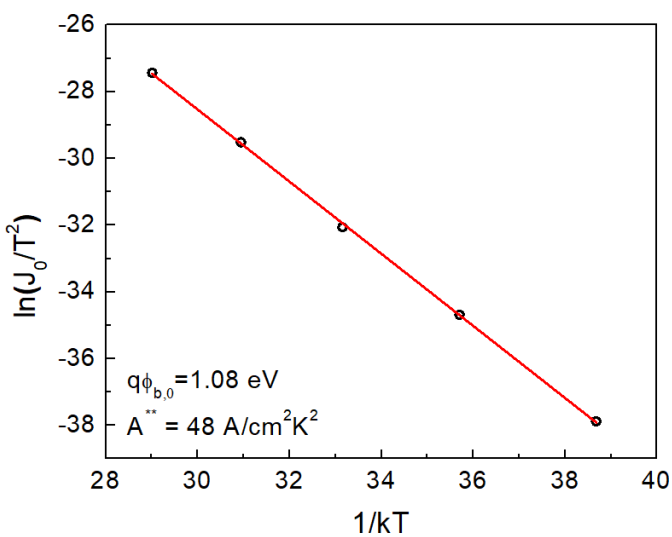

Fig. 4. Richardson plot derived from the forward J-V-T data.

(J)–voltage–temperature (J–V–T) characteristics by means of linear fitting to Richardson's plot shown in Fig. 4 to be 1.08 eV, with Richardson's constant of 48 A · cm^{-2} · K^{-2}. These compare to values of 1.15 eV and 55 A · cm^{-2} · K^{-2} reported by Higashiwaki *et al.* [16] for Pt on Ga_2O_3 drift layers of generally similar characteristics and are in line with previous reports for Au, Ni, and Pt. From these observations, Farzana *et al.* [33] inferred that Fermi-level pinning or the presence of a dielectric layer at the interface in the ideal case did not dominate the Schottky barrier behavior formed with those three metals. Yao *et al.* [34] observed that *I–V* and *C–V* determined SBH values on β-Ga_2O_3 with (201) orientation showed very weak correlation with the metal work functions [10], suggesting the presence of Fermi-level pinning.

Fig. 5 shows the variation of barrier height and ideality factor on temperature for the range 25 °C–125 °C for the 0.2 × 0.3 cm^2 diodes. The barrier height decreases with

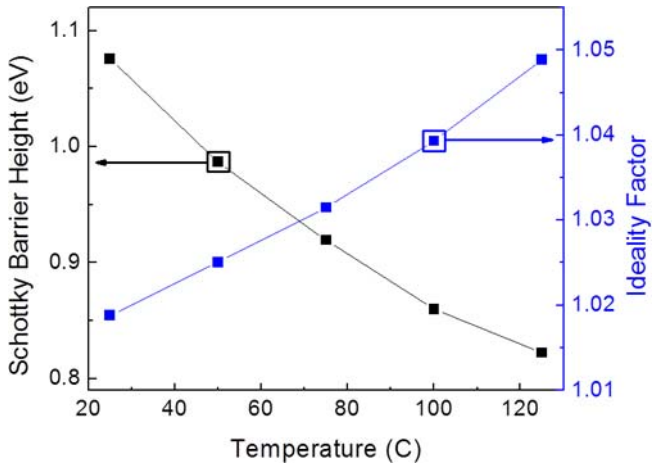

Fig. 5. Temperature dependence of barrier height and ideality factor for 0.2×0.3 cm^2 diode.

temperature, as expected since pure TE would lead to a reduced barrier at elevated temperatures.

The reverse characteristics were taken from dc measurements using the parameter analyzer. These I–V characteristics are shown for room temperature measurements of the four different device sizes in Fig. 6 in both linear (top) and log (bottom) scales. The reverse breakdown voltage (defined as the voltage at which the reverse current was 1 μA $\cdot$ cm^{-2}. This is a more usual definition than where the current sharply increases, since the latter depends on conduction mechanism) of the large area device was small (~15 V) and increased with reduced area to 466 V for the smallest diode active area. This is consistent with the larger devices having an increased probability of containing defects that initiate premature breakdown [35]–[41]. Most previously reported diode rectifiers have had areas of less than 10^{-3} cm^2 and this effect will not be obvious in that situation [7], [17]–[19]. Oshima *et al.* [37] found a spatial correlation between dicing-induced defects and large reverse leakage currents in diodes fabricated in those areas on (001) oriented substrates. Kasu *et al.* [36] reported densities of etch pits above 10^4 cm^{-2} whose presence did not directly correlate with increased reverse leakage current in similar diodes on (001) oriented substrates. Dislocation defects along the [010] direction were found to act as paths for leakage current, while the Si doping did not affect this dislocation-related leakage current. On other orientations, etch pit densities are currently in the range 10^3–6×10^4 cm^{-2} for (201) oriented β-Ga_2O_3 grown by edge-fed defined growth [35]. Both line-shaped etched grooves along the [010] direction and small pits were reported, with the small pits being due to edge dislocations. Thus the orientation of the substrate used determines the sensitivity to defect density. What is clear is the larger the diode active area, the larger the probability of including defects that degrade breakdown voltage. The breakdown voltage of the devices is plotted in the inserts of Fig. 6 (bottom) as a function of top contact area (left) or contact circumference (right). There is a better correlation in the latter case, suggesting that the surface is the dominating contributor to breakdown. It must be remembered that the contact edges of the large

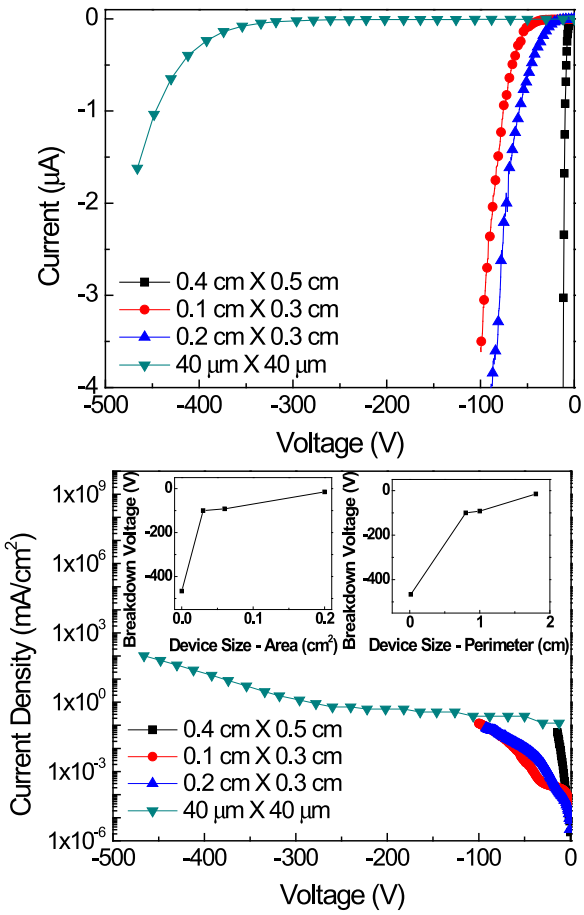

Fig. 6. Reverse current at room temperature as a function of diode size in (top) linear or (bottom) log scales. Inserts are the reverse breakdown voltage at room temperature as a function of either diode area or circumference.

area devices are sharp, while the corners of the contacts for the 40×40 μm^2 devices are rounded, with less tendency to break down at the edges, but the data are still a useful indicator that edge termination techniques to reduce field crowding are desirable.

The on-state resistance values ranged from 5.9×10^{-4} to 0.26 $\Omega \cdot$ cm^2 for areas in the corresponding range 1.6×10^{-5}–0.2 cm^2, which is comparable to that expected from the relation

$$R_{\mathrm{ON}} = \frac{W_D}{e} \mu N_D$$

where W_D is the depletion layer thickness, e is the electronic charge, μ is the electron mobility and N_D is the background n-type doping level of the Ga_2O_3 epitaxial layer. The values are also comparable to those reported by Sasaki *et al.* [14] (4.30–7.85 m$\Omega \cdot$ cm^{-2}) and Higashiwaki *et al.*[7], [16] (2.4–3 m$\Omega \cdot$ cm^{-2}) for their particular size rectifiers. The figure-of-merit V_B^2/R_{ON} varied from 865–3.68×10^8W cm^{-2} for the range of diode areas investigated, as listed in Table I. The high end of this range of power densities is already consistent with values for GaN and SiC and will increase as the technology matures and both high forward currents and high reverse breakdown voltages are achieved on the same devices. Note that Ga_2O_3 rectifiers at a given voltage will have

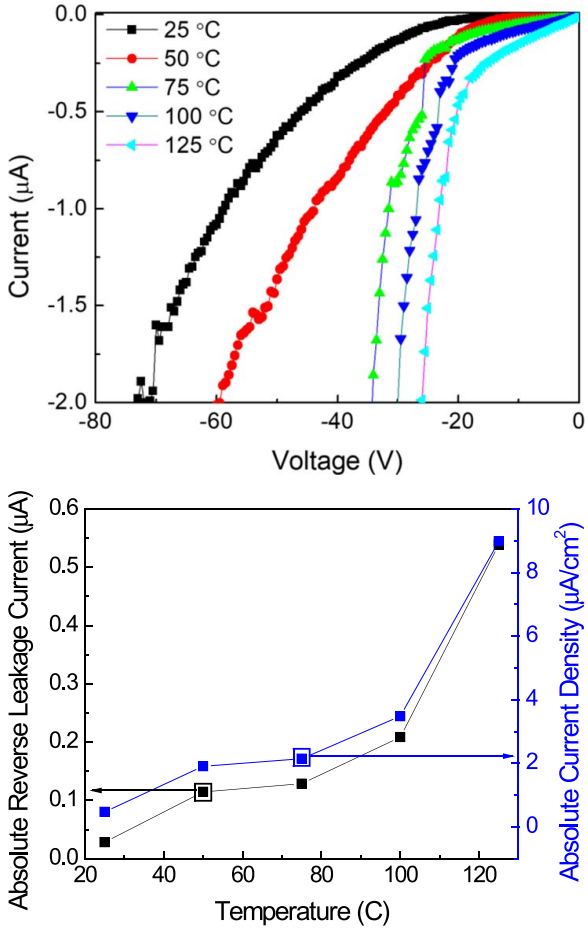

Fig. 7. Reverse *I–V* characteristics as a function of temperature for a 0.2 × 0.3 cm^2 diode (top) and reverse currents and current densities at a fixed bias of 20 V (bottom).

theoretical on-resistances more than an order of magnitude lower than Si and a factor of 2 lower than SiC, while at a given on-resistance, the theoretical breakdown has the same degree of enhancement in both cases [6]–[11]. The breakdown field is more than double the theoretical limits of SiC and GaN the Baliga figure-of-merit commonly used to evaluate the suitability of a material for power switching devices predicts more than triple their power device performance [10].

As shown in Fig. 7 (top) the reverse breakdown voltage, V_B, was found to decrease with measurement temperature T, according to the linear reverse breakdown relationship as

$$V_{\mathrm{RB}} = V_{\mathrm{RB0}} + \beta(T - T_0)$$

where the temperature coefficient β was determined to be −0.45 V/K for Ni in our devices [32]. For simple Schottky diodes with even smaller area than the smallest used here, Ahn *et al.* [32] reported temperature coefficient β of −4 m · V/K for Ni/Au and −0.1 m · V/K for Pt/Au. It is typical of newer power materials technologies that β tends to get smaller as growth and process methods are optimized and also that it will be a function of device area. Fig. 8 (bottom) shows the reverse leakage current and current density as a function of temperature for the 0.2 × 0.3 cm^2 diode at a bias of 20 V, emphasizing the strong activation with temperature.

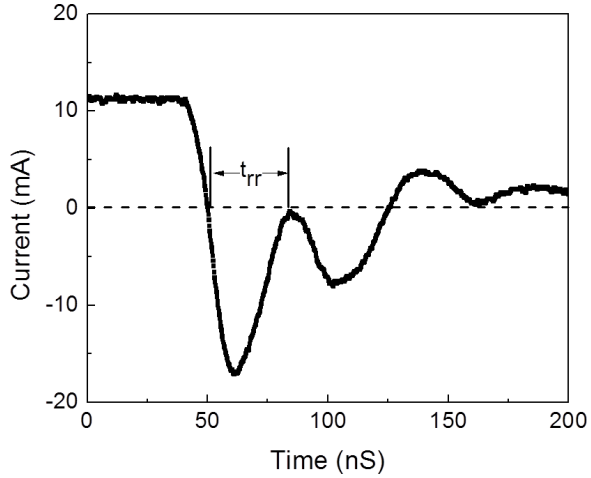

Fig. 8. Reverse recovery characteristic of 0.2 × 0.3 cm^2 diode upon switching from 1-V forward current to −10-V reverse bias.

We also measured the reverse recovery characteristics when switching from +1 V to a range of reverse biases and found recovery times of order 20–30 ns for these rectifiers, as shown in Fig. 8. We have reported previously in electron irradiated rectifiers that the reverse recovery shows little change with radiation dose [42], since the minority carrier lifetime (which controls the carrier storage time in the intrinsic layer) is already small in Ga_2O_3.

IV. Summary and Conclusion

Ga_2O_3 rectifiers with areas of 0.03 cm^2 fabricated on low carrier density epitaxial layers on bulk substrates produced 2.2 A of forward current at 2 V under single sweep conditions, the largest on-state current ever reported for a Ga_2O_3 rectifier. Future work should focus on implementing optimized edge termination approaches, and continuing to lower the background doping level and defect density in the epitaxial Ga_2O_3, which obviously includes optimizing the surface preparation of the starting substrate. The existing material exhibits a negative temperature coefficient for V_B, but this is expected to be lower in low defect substrates. For example, with an pit density of 10^3, the 0.1 cm × 0.3 cm diode would have 30 pits. The 40 μm × 40 μm diode would have 0.16 pits (less than 1); some of the smaller diodes may then not have any pits on them. Therefore the breakdown voltage of 40 μm × 40 μm diode is much higher than that of the larger diodes. This is usually the result of defects that enhance multiplication, leading to reduced breakdown and has been reported previously in the early stage development of SiC and GaN power electronics. The impact ionization coefficients (α_p) for holes measured near defects were found to be higher than those measured at a non-defective regions [43]. Also, the values measured near defects were was found to increase with increasing temperature in contrast with a defect free diode where α_p decreased with the increasing temperature, clearly indicating that the defects produce the observed negative temperature coefficient of breakdown voltage.

The viability of Ga_2O_3 rectifiers in most applications depends on making very large area devices with high V_B,

while retaining low V_F and R_{ON}. The low thermal conductivity of Ga_2O_3 means that packaging approaches must include cooling by both topside and backside heat extraction [10]. This may need to go beyond heat sinks to wafer transfer onto supporting substrates with higher thermal and electrical conductivities. Commercial SiC MOSFET switches and Schottky diodes are available up to 12 kV, 60 A at 20 kHz, operational to 50 kHz at lower currents [12]. Even higher voltages of 15 kV (at 5 kHz) with SiC IGBT switches and SiC PiN diodes. SiC Schottky barrier diodes are commonly used in power factor correction circuits and IGBT power modules. SiC power devices are used in the U.S. Navy DDG 1000 Zumwalk Class destroyer to supply 78 MW at 4160 V. GaN 1200 V parts first appeared in 2012 and enable operation beyond 2 MHz, which enables large step down ratios in buck converters and decreases passive components sizes [12]. This paper has shown the promise of Ga_2O_3 to operate at high current, in addition to the previous demonstrations of high reverse voltage.

Acknowldgment

The authors would like to thank Dr. Kohei Sasaki from Tamura Corporation, Sayama, Japan.

References

[1] A. Kuramata, K. Koshi, S. Watanabe, Y. Yamaoka, T. Masui, and S. Yamakoshi, "High-quality β-Ga_2O_3 single crystals grown by edge-defined film-fed growth," *Jpn. J. Appl. Phys.*, vol. 55, no. 12, p. 1202A2, 2016, doi: 10.7567/JJAP.55.1202A2.

[2] Z. Galazka *et al.*, "Scaling-up of bulk β-Ga_2O_3 single crystals by the Czochralski method," *ECS J. Solid State Sci. Technol.*, vol. 6, no. 2, pp. 3007–3010, 2017, doi: 10.1149/2.0021702jss.

[3] M. J. Tadjer *et al.*, "Structural, optical, and electrical characterization of monoclinic β-Ga_2O_3 grown by MOVPE on sapphire substrates," *J. Electron. Mater.*, vol. 45, no. 4, pp. 2031–2036, 2016, doi: 10.1007/s11664-016-4346-3.

[4] S. Rafique *et al.*, "Heteroepitaxy of N-type β-Ga_2O_3 thin films on sapphire substrate by low pressure chemical vapor deposition," *Appl. Phys. Lett.*, vol. 109, no. 13, p. 132103, 2016, doi: 10.1063/1.4963820.

[5] M. Baldini, M. Albrecht, A. Fiedler, K. Irmscher, R. Schewski, and G. Wagner, "Si- and Sn-doped homoepitaxial β-Ga_2O_3 layers grown by MOVPE on (010)-oriented substrates," *ECS J. Solid State Sci. Technol.*, vol. 6, no. 2, pp. Q3040–Q3044, 2017, doi: 10.1149/2.0081702jss.

[6] H. Von Wenckstern, "Group-III sesquioxides: Growth, physical properties and devices," *Adv. Electron. Mater.*, vol. 3, no. 9, p. 1600350, 2017, doi: 10.1002/aelm.201600350.

[7] M. Higashiwaki *et al.*, "Recent progress in Ga_2O_3 power devices," *Semicond. Sci. Technol.*, vol. 31, no. 3, p. 034001, 2016, doi: 10.1088/0268-1242/31/3/034001.

[8] S. J. Pearton *et al.*, "A review of Ga_2O_3 materials, processing, and devices," *Appl. Phys. Rev.*, vol. 5, no. 1, p. 011301, 2018, doi: 10.1063/1.5006941.

[9] M. A. Mastro, A. Kuramata, J. Calkins, J. Kim, F. Ren, and S. J. Pearton, "Perspective—Opportunities and future directions of Ga_2O_3," *ECS J. Solid State Sci. Technol.*, vol. 6, no. 5, pp. 356–359, 2017, doi: 10.1149/2.0031707jss.

[10] M. Higashiwaki and G. H. Jessen, "The dawn of gallium oxide microelectronics," *Appl. Phys. Lett.*, vol. 112, no. 6, p. 060401, 2018, doi: 10.1063/1.5017845.

[11] K. J. Chen *et al.*, "GaN-on-Si power technology: Devices and applications," *IEEE Trans. Electron Devices*, vol. 64, no. 3, pp. 779–795, Mar. 2017, doi: 10.1109/TED.2017.2657579.

[12] A. Q. Huang, "Power semiconductor devices for smart grid and renewable energy systems," *Proc. IEEE*, vol. 105, no. 11, pp. 2019–2047, Nov. 2017, doi: 10.1109/JPROC.2017.2687701.

[13] M. Mohamed, K. Irmscher, C. Janowitz, Z. Galazka, R. Manzke, and R. Fornari, "Schottky barrier height of Au on the transparent semiconducting oxide β-Ga_2O_3," *Appl. Phys. Lett.*, vol. 101, no. 13, p. 132106, 2012, doi: 10.1063/1.4755770.

[14] K. Sasaki, M. Higashiwaki, A. Kuramata, T. Masui, and S. Yamakoshi, "Ga_2O_3 Schottky barrier diodes fabricated by using single-crystal β–Ga_2O_3(010) substrates," *IEEE Electron Device Lett.*, vol. 34, no. 4, pp. 493–495, Apr. 2013, doi: 10.1109/LED.2013.2244057.

[15] T. Oishi, Y. Koga, K. Harada, and M. Kasu, "High-mobility β-$Ga_2O_3(\bar{2}01)$ single crystals grown by edge-defined film-fed growth method and their Schottky barrier diodes with Ni contact," *Appl. Phys. Express*, vol. 8, no. 3, p. 031101, 2015, doi: 10.7567/APEX.8.031101.

[16] M. Higashiwaki *et al.*, "Temperature-dependent capacitance–voltage and current–voltage characteristics of Pt/Ga_2O_3 (001) Schottky barrier diodes fabricated on n^-–Ga_2O_3 drift layers grown by halide vapor phase epitaxy," *Appl. Phys. Lett.*, vol. 108, no. 13, p. 133503, 2016, doi: 10.1063/1.4945267.

[17] J. Yang *et al.*, "High reverse breakdown voltage Schottky rectifiers without edge termination on Ga_2O_3," *Appl. Phys. Lett.*, vol. 110, no. 19, p. 192101, 2017, doi: 10.1063/1.4983203.

[18] J. Yang, S. Ahn, F. Ren, S. J. Pearton, S. Jang, and A. Kuramata, "High breakdown voltage (−201) β-Ga_2O_3 Schottky rectifiers," *IEEE Electron Device Lett.*, vol. 38, no. 7, pp. 906–909, Jul. 2017, doi: 10.1109/LED.2017.2703609.

[19] K. Konishi, K. Goto, H. Murakami, Y. Kumagai, A. Kuramata, S. Yamakoshi, and M. Higashiwaki, "1-kV vertical Ga_2O_3 field-plated Schottky barrier diodes," *Appl. Phys. Lett.*, vol. 110, no. 10, p. 103506, 2017, doi: 10.1063/1.4977857.

[20] M. H. Wong, K. Sasaki, A. Kuramata, S. Yamakoshi, and M. Higashiwaki, "Field-plated Ga_2O_3 MOSFETs with a breakdown voltage of over 750 V," *IEEE Electron Device Lett.*, vol. 37, no. 2, pp., pp. 212–215, Feb. 2016, doi: 10.1109/LED.2015.2512279.

[21] K. Sasaki, Q. T. Thieu, D. Wakimoto, Y. Koishikawa, A. Kuramata, and S. Yamakoshi, "Depletion-mode vertical Ga_2O_3 trench MOSFETs fabricated using Ga_2O_3 homoepitaxial films grown by halide vapor phase epitaxy," *Appl. Phys. Express*, vol. 10, no. 12, p. 124201, 2017, doi: 10.7567/APEX.10.124201.

[22] A. J. Green *et al.*, "3.8-MV/cm breakdown strength of MOVPE-grown Sn-doped β-Ga_2O_3 MOSFETs," *IEEE Electron Device Lett.*, vol. 37, no. 7, pp. 902–905, Jul. 2016, doi: 10.1109/LED.2016.2568139.

[23] N. A. Moser *et al.*, "High pulsed current density β-Ga_2O_3 MOSFETs verified by an analytical model corrected for interface charge," *Appl. Phys. Lett.*, vol. 110, no. 14, p. 143505, 2017, doi: 10.1063/1.4979789.

[24] H. Zhou, K. Maize, G. Qiu, A. Shakouri, and P. D. Ye, "β-Ga_2O_3 on insulator field-effect transistors with drain currents exceeding 1.5 A/mm and their self-heating effect," *Appl. Phys. Lett.*, vol. 111, no. 9, p. 092102, 2017, doi: 10.1063/1.5000735.

[25] K. D. Chabak *et al.*, "Enhancement-mode Ga_2O_3 wrap-gate fin field-effect transistors on native (100) β-Ga_2O_3 substrate with high breakdown voltage," *Appl. Phys. Lett.*, vol. 109, no. 21, p. 213501, 2016, doi: 10.1063/1.4967931.

[26] M. H. Wong, Y. Nakata, A. Kuramata, S. Yamakoshi and M. Higashiwaki, "Enhancement-mode Ga_2O_3 MOSFETs with Si-ion-implanted source and drain," *Appl. Phys. Express*, vol. 10, no. 4, p. 041101, 2017, doi: 10.7567/APEX.10.041101.

[27] E. Ahmadi, O. S. Koksaldi, X. Zheng, T. Mates, Y. Oshima, U. K. Mishra and J. S. Speck, "Demonstration of β-$(Al_x\ Ga_{1-x})_2O_3$/β-Ga_2O_3 modulation doped field-effect transistors with Ge as dopant grown via plasma-assisted molecular beam epitaxy," *Appl. Phys. Express*, vol. 10, no. 7, p. 071101, 2017, doi: 10.7567/APEX.10.071101.

[28] S. Krishnamoorthy *et al.*, "Modulation-doped β-$(Al_{0.2}Ga_{0.8})_2O_3$/Ga_2O_3 field-effect transistor," *Appl. Phys. Lett.*, vol. 111, no. 2, p. 023502, 2017, doi: 10.1063/1.4993569.

[29] A. J. Green *et al.*, "β-Ga_2O_3 MOSFETs for radio frequency operation," *IEEE Electron Device Lett.*, vol. 38, no. 6, pp. 790–793, Jun. 2017, doi: 10.1109/LED.2017.2694805.

[30] T. Oshima *et al.*, "Carrier confinement observed at modulation-doped β-$(Al_xGa_{1-x})_2O_3$/Ga_2O_3 heterojunction interface," *Appl. Phys. Express*, vol. 10, no. 3, p. 035701, 2017, doi: 10.7567/APEX.10.035701.

[31] G. T. Heydt and B. J. Skromme, "Applications of high-power electronic switches in the electric power utility industry and the needs for high-power switching devices," in *Proc. Mat. Res. Soc. Symp.*, vol. 483, 1998, p. 3.

[32] S. Ahn, F. Ren, L. Yuan, S. J. Pearton, and A. Kuramata, "Temperature-dependent characteristics of Ni/Au and Pt/Au Schottky diodes on β-Ga_2O_3," *ECS J. Solid State Sci. Technol.*, vol. 6, no. 1, pp. P68–P72, 2017, doi: 10.1149/2.0291701jss.

[33] E. Farzana, Z. Zhang, P. K. Paul, A. R. Arehart, and S. A. Ringel, "Influence of metal choice on (010) β-Ga_2O_3 Schottky diode properties," *Appl. Phys. Lett.*, vol. 110, no. 20, p. 202102, 2017, doi: 10.1063/1.4983610.

[34] Y. Yao, R. Gangireddy, J. Kim, K. K. Das, R. F. Davis, and L. M. Porter, "Electrical behavior of β-Ga_2O_3 Schottky diodes with different Schottky metals," *J. Vac. Sci. Technol. B*, vol. 35, no. 3, p. 03D113, 2017, doi: .10.1116/1.4980042.

[35] O. Ueda *et al.*, "Structural evaluation of defects in β-Ga_2O_3 single crystals grown by edge-defined film-fed growth process," *Jpn. J. Appl. Phys*, vol. 55, no. 12, p. 1202BD, 2016, doi: 10.7567/JJAP.55.1202BD.

[36] M. Kasu *et al.*, "Crystal defects observed by the etch-pit method and their effects on Schottky-barrier-diode characteristics on ($\bar{2}01$) β-Ga_2O_3," *Jpn. J. Appl. Phys.*, vol. 56, no. 9, p. 091101, 2017, doi: 10.7567/JJAP.56.091101.

[37] T. Oshima *et al.*, "Electrical properties of Schottky barrier diodes fabricated on (001) β-Ga_2O_3 substrates with crystal defects," *Jpn. J. Appl. Phys.*, vol. 56, no. 8, p. 086501, 2017, doi: 10.7567/JJAP.56.086501.

[38] K. Nakai, T. Nagai, K. Noami, and T. Futagi, "Characterization of defects in β-Ga_2O_3 single crystals," *Jpn. J. Appl. Phys.*, vol. 54, p. 051103, 2015, doi: .10.7567/JJAP.54.051103.

[39] K. Hanada *et al.*, "Observation of nanometer-sized crystalline grooves in as-grown β-Ga_2O_3 single crystals," *Jpn. J. Appl. Phys.*, vol. 55, no. 3, pp. 030303-1–030303-5, 2016, doi: .10.7567/JJAP.55.030303.

[40] K. Hanada *et al.*, "Origins of etch pits in β-Ga_2O_3(010) single crystals," *Jpn. J. Appl. Phys.*, vol. 55, no. 12, p. 1202BG, 2016, doi: 10.7567/JJAP.55.1202BG.

[41] M. Kasu *et al.*, "Relationship between crystal defects and leakage current in β-Ga_2O_3 Schottky barrier diodes," *Jpn. J. Appl. Phys.*, vol. 55, no. 12, pp. 1202BB-1–1202BB-4, 2016, doi: 10.7567/.JJAP.55.1202BB.

[42] J. Yang, F. Ren, S. J. Pearton, G. Yang, J. Kim, and A. Kuramata, "1.5 MeV electron irradiation damage in β-Ga_2O_3 vertical rectifiers," *J. Vac. Sci. Technol. B*, vol. 35, no. 3, p. 031208, 2017, doi: 10.1116/1.4983377.

[43] R. Raghunathan and B. J. Baliga, "Role of defects in producing negative temperature dependence of breakdown voltage in SiC," *Appl. Phys. Lett.*, vol. 72, no. 24, pp. 3196–3198, 1998, doi: .10.1063/1.121591.

Jiancheng Yang is a Graduate Student Fellow with the Department of Chemical Engineering, University of Florida, Gainesville, FL, USA. His current research interests include the fabrication and characterization of compound semiconductor devices and biosensors.

Fan Ren (F'10) is a Distinguished Professor at the University of Florida (UF), Gainesville, FL, USA. He joined UF in 1997 after 12 years at AT&T Bell Laboratories, Murray Hill, NJ,USA.

Prof. Ren is a fellow of the Electrochemical Society, the Materials Research Society, the Society of Photographic Instrumentation Engineers, the American Physical Society, and the American Vacuum Society.

Steve J. Pearton (F'01) received the Ph.D. degree in physics from the University of Tasmania, Hobart, TAS, Australia.

He was with AT&T Bell Laboratories, Murray Hill, NJ, USA, from 1994 to 2004. He is a Distinguished Professor at the University of Florida, Gainesville, FL, USA.

Dr. Pearton was a recipient of the 2007 J. J. Ebers Award from IEEE.

Akito Kuramata was born in Itoigawa, Japan, in 1963. He received the B.E. degree from Kyoto University, Kyoto, Japan, in 1986.

He joined Fujitsu Laboratories Ltd., Atsugi, Japan. He moved to Tamura Corporation, Sayama, Japan, in 2008. He established Novel Crystal Technology, Inc., Sayama, in 2016. His current research interests include crystal growth and device process for laser diodes, optical detectors and transistors.